COMPARISON OF TEXTURE FEATURES FOR HUMAN EMBRYONIC STEM CELLS WITH BIO-INSPIRED MULTI-CLASS SUPPORT VECTOR MACHINE

Benjamin X. Guan, Bir Bhanu, Prue Talbot, Sabrina Lin* and Nikki Weng**

Center for Research in Intelligent Systems, *Stem Cell Center
University of California, Riverside, CA 92521, USA
Email:{xguan001, bhanu}@ee.ucr.edu, {prue.talbot, sabrina.lin, jweng002}@ucr.edu

ABSTRACT

Determining the meaningful texture features for human embryonic stem cells (hESC) is important in the development of online hESC classification system. This paper proposes the use of novel support vector machine with bio-inspired one-against-all (OAA) multi-class structural and statistical Gabor descriptors for hESC classification. It investigates the statistical histogram information at four different orientations and two different window sizes of the Gabor filter. It demonstrates that statistical Gabor features are more accurate and reliable than a conventional histogram based features.

Index Terms— Classification, Gabor filter, Human embryonic stem cells (hESC), One-against-all (OAA)

1. INTRODUCTION

Human embryonic stem cells (hESC) are derived from the inner cell mass of developing blastocysts and can be maintained indefinitely in vitro in a pluripotent state [1]. Because of their ability to self-renew and their potential to differentiate into any cell type, hESC provide a unique resource for regenerative medicine, basic research on human prenatal development, and toxicological testing of drugs and environmental chemicals [2][3]. In the current studies, biologists have used time-lapse imaging of cells to monitor dynamic behavior of hESC in different experimental conditions [4][5][6]. While performing these studies, we observed that hESC undergo dynamic blebbing during the first 20-60 minutes after plating, and if they do not attach to their substrate during the first hour after plating, they undergo apoptosis. Due to the fact that dynamic blebbing occurs in the first hour of incubation, it can be used to evaluate hESC health following plating, and it can also serve as the basis for a rapid toxicological assay. Although it takes little time to perform the blebbing assay, manual analysis of the resulting video data is time-consuming and subjective. Therefore, analysis tool such as a hESC classification system is essential for quantified analysis. An automated classification system can help biologists to identify interesting behaviors of hESC easily. It can provide the biologists the statistics of different types of stem cell in the current analysis. It can assist the biologists to draw a conclusion for a particular experiment.

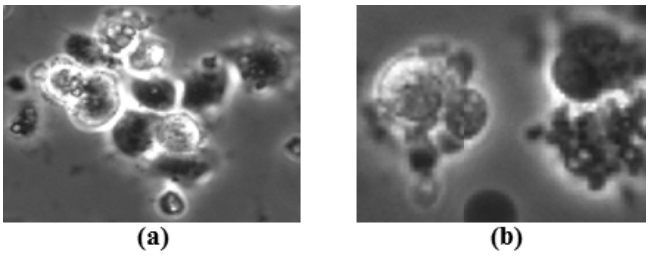

Fig. 1 (a) Cell colony; (b) close-knit cells.

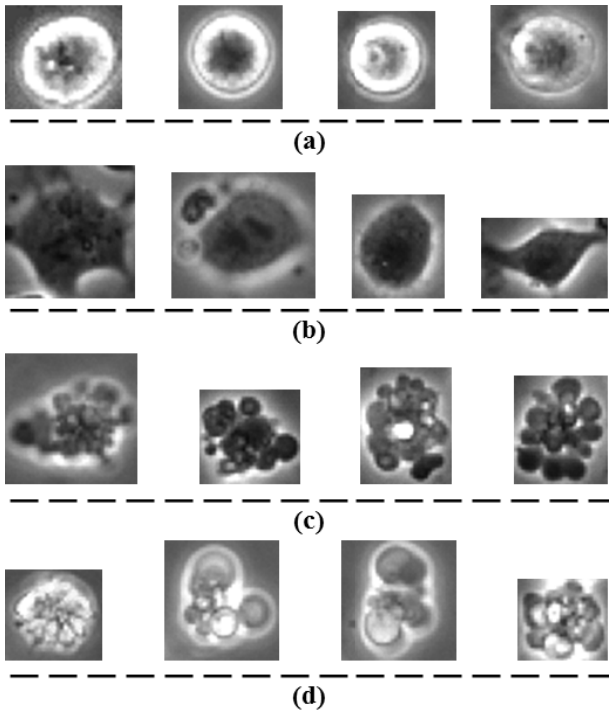

Fig. 2 (a) Unattached cells; (b) attached cells; (c) dynamically blebbing cells; (d) apoptotically blebbing cells.

A hESC video is made up by frames of phase contrast image. Each frame comprises of two major categories. One is the multi-cell category shown in Fig. 1, the other is the single cell category shown in Fig. 2. There are two types of

multi-cells: 1) cell colony; 2) close-knit cells. Cell colony comprises of two or more single cells. The close-knit cells consist of two or more individual components. Each component can either be a single cell or a cell colony. The four intrinsic types of single cell are: 1) unattached cell (U); 2) attached cell (A); 3) dynamically blebbing cell (D); 4) apoptotically blebbing cell (AP). Since the assays are formed by the four intrinsic cell types, the classification of these cell types is important. Therefore, this paper focuses on the classification of the four intrinsic types of stem cell.

2. RELATED WORKS

There is no existing study for the automated classification of hESC. However, there are many classification studies that use features based on local binary patterns (LBP), local phase quantization (LPQ), and Gabor filtering. The simplest LBP compare each of its eight neighbors' intensity values with its center intensity value [7]. The neighboring pixel has a value of 1 if its intensity value is greater than the center intensity value. Otherwise, the neighboring pixel has a value of 0. LPQ obtain local frequency coefficients for each pixel at certain frequencies [8]. The coefficients are then quantized and translated into a histogram. The Gabor filter is a 2D Gaussian kernel function that is modulated by a sinusoidal plane wave at certain frequency and orientation [9][10]. A histogram is generally generated from the Gabor filtered image as a feature vector. Conventionally, a histogram is either a histogram of the entire image or a cascaded histogram from smaller windows of the image. However, resizing the dataset is needed for a cascaded histogram. Since our dataset images have an average size of 58 by 60 pixels, we use the histogram of the entire image in this paper for all histogram based comparison methods.

TABLE 1
AVERAGE CROSS-CORRELATION (CC) VALUES FOR CELL TYPES SHOWN IN FIGURE 2 (GRAY SCALE ONLY)

Histogram Based	**U**	**A**	**D**	**AP**
U	*0.6578*	0.1064	0.3184	**0.5982**
A	0.1064	*0.7468*	**0.6187**	0.1531
D	0.3184	**0.6187**	*0.6960*	0.3945
AP	**0.5982**	0.1531	0.3945	*0.7365*

(a)

Statistics Based	**U**	**A**	**D**	**AP**
U	*0.9992*	0.9981	0.9984	**0.9990**
A	0.9981	*0.9996*	**0.9988**	0.9979
D	0.9984	**0.9988**	*0.9985*	0.9982
AP	**0.9990**	0.9979	0.9982	*0.9992*

(b)

Underline & italics denote correlation and bold denotes highest CC value in the row.

Our contribution in this paper is to introduce a binary support vector machine (SVM) with a bio-inspired one-against-all (OAA) model for multi-class classification [11][12]. We use statistical Gabor wavelet for multi-class classification. We investigate the Gabor filter parameters and find out parameters that yield the best performance in multi-class classification for the four intrinsic cell types. We compared the conventional histogram based features and the statistics based features in this paper.

3. TECHNICAL APPROACH

In this section, we first explain our motivation and the problem formulation. We also briefly explain Gabor filter in subsection 3.2. We then elaborate on the statistical Gabor descriptors for multi-class classification.

3.1. Motivation and Problem Formulation

The four intrinsic hESC considered in this paper have characteristics such as roundedness, elongatedness and bubble-like shape. Texture is important to distinguish these cell types, so we use texture features in this paper. Since Gabor filters give useful descriptors at different window sizes, frequencies and orientations, we investigated the Gabor filter for classification of hESC. For the choice of a classifier, we have used the SVM. The SVM is a binary decision classifier. As a result, we also adopted OAA model for multi-class classification. The OAA model is the most efficient way to use SVM for multi-class classification [12].

The OAA model for multi-class classification is bio-inspired. Based on biological insights, the unattached cells are round, and they are brighter in intensity than attached and dynamically blebbing cells. As shown in Fig. 2, unattached and apoptotically blebbing cells have high intensity values while attached and dynamically blebbing cells are darker in intensity. Table 1 shows support for our biological insights. The cross-correlation (CC) value between cell types using either the gray scale histogram based or statistics based features shows that highest CC value among cell types separates the 4 cell types into 2 groups. Since apoptotically blebbing cell has a higher average CC value than unattached cell, the positive and negative sets at level 0 of OAA hierarchy is given by: {U} and {A, D, AP}.

With the aforementioned facts, we deduced a bio-inspired structure for one-against-all classification method. Fig. 3 shows how the OAA method is constructed with SVM as a fundamental classifier. If the input image is recognized as negative sample, then further classification is needed. The positive and negative samples at each level are chosen based on how a particular cell type is prevalently different from the rest of other cell types.

Since we are developing an online classification system, accuracy, reliability and low time complexity are essential. The fewer the feature descriptors, the lower the

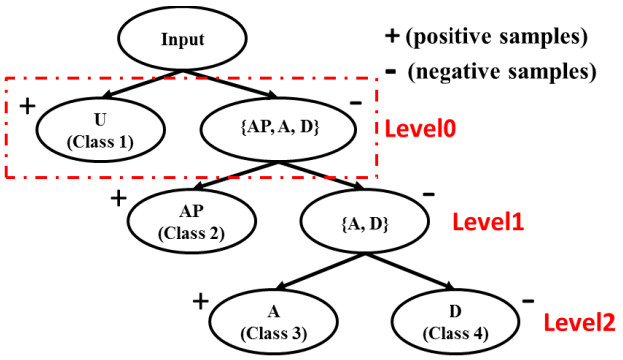

Fig. 3 Bio-inspired one-against-all (OAA) model for multi-class classification.

time complexity. Therefore, we only considered five key statistical features; 1) mean; 2) mode; 3) entropy; 4) variance; 5) energy.

3.2. Gabor Filter

Gabor filtering is a convolution of an image, I , with a 2D Gaussian kernel, G , that is modulated by a sinusoidal plane wave. The Gaussian equation is shown in equation (1). The modulation, M, is shown in equation (2). The final modulated Gabor equation, G_M, is shown in equation (3) [9].

$$G(x,y) = \frac{1}{2\pi s_x s_y} e^{-\frac{1}{2}\left(\left(\frac{x}{s_x}\right)^2 + \left(\frac{y}{s_y}\right)^2\right)} \quad (1)$$

$$M(x,y,f,\theta) = \cos\left(2\pi f\left(x\cos(\theta) + y\sin(\theta)\right)\right) \quad (2)$$

$$G_M(x,y,f,\theta) = G(x,y)M(x,y,f,\theta) \quad (3)$$

Note that x ∈ $[-S_x, S_x]$, y ∈ $[-S_y, S_y]$, S_x and S_y are standard deviation in the x and y direction, f is the frequency of sinusoidal wave, and θ is the orientation. The final filtered image, I_G , is obtained by convolution as shown in below [9][10]. (Note that * denotes convolution.)

$$I_G = I * G_M \quad (4)$$

3.3. Statistical Descriptors

The statistical descriptors are derived directly from the histogram of the image with or without filtering. The following equations show the statistics based descriptors that are derived from the histogram of an image [13].

$$\mu = \frac{1}{S}\sum_{n=0}^{N} nH(n) \quad (5)$$

$$\psi = \max_n\left(\mathrm{H(n)}\right) \quad (6)$$

$$\rho = -\sum_{n=0}^{N} \frac{H(n)}{S}\log_2\left(\frac{H(n)}{S} + 1\right) \quad (7)$$

$$\sigma^2 = \frac{1}{S}\sum_{n=0}^{N} H(n)(n-\mu)^2 \quad (8)$$

$$\phi = \frac{\sum_{n=0}^{N}\left(H(n)\right)^2}{\left(\sum_{n=0}^{N} H(n)\right)^2} \quad (9)$$

where H is the histogram of the image and n is an index which spans from 0 to N. In this paper, N is 255. S is the total number of pixels in the image. μ, ψ, ρ, σ^2 and ϕ are mean, mode, entropy, variance and energy of the image. The statistical descriptors of all the texture filters mentioned in this paper are obtained using the above equations.

4. EXPERIMENTAL RESULTS

4.1. Data

All time lapse videos were obtained with a BioStation IM under 20x objective [14]. Each video frame was taken roughly 2 minutes apart for the purpose of data variation from frame to frame. The frames in the video were phase contrast images with 600 x 800 resolution. Each frame was then decomposed into smaller images by a cell region detection algorithm [15]. The four intrinsic cell types were then identified by an expert stem cell biologist from the pool of images, and datasets were generated from 8 videos.

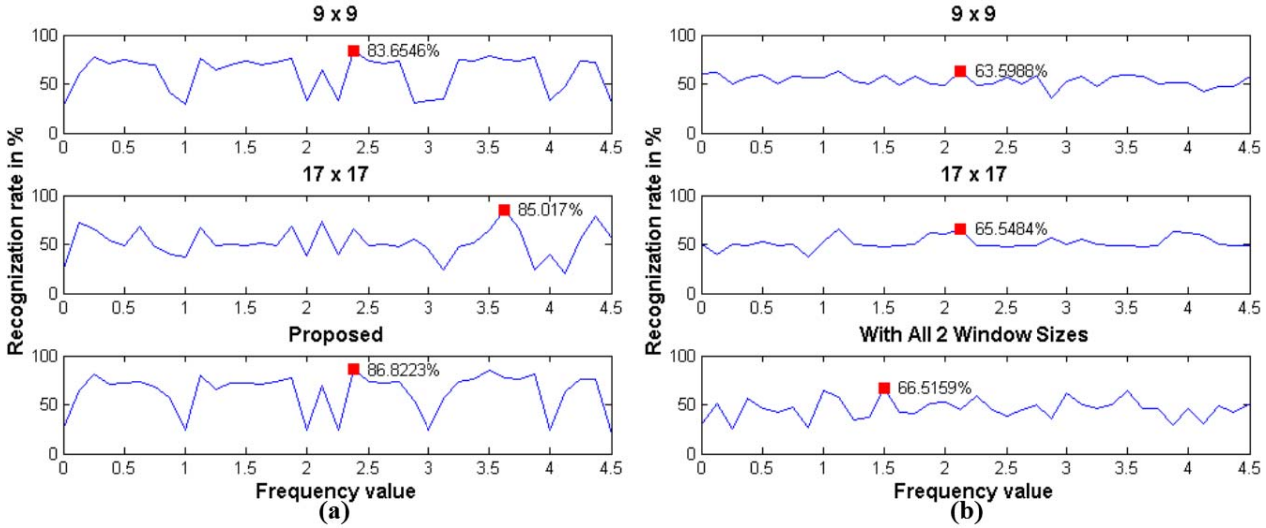

Fig. 4 (a) Methods with Gabor statistics for each window size under different frequencies; (b) Methods with Gabor histogram for each window size under different frequencies. (red square denotes optimal point.)

TABLE 2: TEN-FOLD COMPARISON RESULTS IN THIS PAPER (4 ORIENTATIONS ARE USED FOR ALL GABOR METHODS)

Features	Unattached	AP Blebbing	Attached	Dynam. Blebbing	ARR
Gray Scale Histogram	29.04%	94.91%	0.00%	100.00%	55.99%
Gray Scale Statistics	0.00%	0.94%	0.00%	95.00%	23.99%
LBP Histogram	34.11%	11.70%	0.00%	97.75%	35.89%
LBP Statistics	0.68%	5.85%	5.63%	83.50%	23.92%
LPQ Histogram	43.56%	24.15%	0.00%	100.00%	41.93%
LPQ Statistics	1.78%	3.58%	18.16%	76.25%	24.94%
Gabor Histogram (9x9)	70.41%	86.42%	0.00%	93.75%	62.64%
Gabor Statistics (9x9)	78.49%	87.17%	71.55%	97.50%	83.68%
Gabor Histogram (17x17)	82.74%	74.34%	0.00%	99.00%	64.02%
Gabor Statistics (17x17)	86.58%	80.38%	76.89%	100.00%	85.96%
Gabor Wavelet Histogram*	62.88%	87.74%	0.00%	99.75%	62.59%
Proposed*	**78.08%**	**90.38%**	**78.25%**	**100.00%**	**86.68%**

*** denotes windows 9 x 9 and 17 x 17 are used. AP denotes apoptotically, and ARR denotes average recognition rate.**

There was no preprocessing on the dataset images, and their average size is about 58 by 60 pixels. The test datasets had 269 images with 73 images of unattached cell, 103 images of attached cell, 40 images of dynamically blebbing cell and 53 images of apoptotically blebbing cell. The training datasets had a total of 120 images with 30 images for each cell type.

4.2. Parameters

For the Gabor filter, we used 4 orientations and 2 different window sizes [10]. The orientations in degrees were 0, 45, 90 and 135. The window sizes were 9 x 9 and 17 x 17. The frequencies were learned with search from 0 to 4.5 with a 0.125 step size [9]. Note that we used 4 orientations in each window to construct either a histogram based or statistics based descriptor. The optimal frequencies for the Gabor methods are selected when the average recognition rate is achieved and it is shown in Fig. 4. The proposed method used all orientations and window sizes for the descriptors. The frequencies used in the histogram based methods were 2.125, 2.125 and 1.5 for 9 x 9, 17 x 17 and method with all window sizes. For the Gabor statistics based descriptors, we used frequencies 2.375, 3.625 and 2.375 for 9 x 9, 17 x 17 and the proposed. For the LBP, we used 8 neighbors [7]. For the LPQ, the default parameters had the window size of 3 x 3 and decorrelation value of 1 [8].

4.3. Results

We compared the proposed method with histogram and statistics based methods in gray scale, LBP, LPQ and Gabor features at different window sizes with four orientations. The Gabor histogram based method with 2 window sizes and 4 orientations was also compared. As shown in Table 2, the proposed method yields ten-fold accuracies of 78.08% for unattached cell, 90.38% for apoptotically blebbing cell, 78.25% for attached cell and 100.00% for dynamically blebbing cell. The proposed method outperformed all other methods in the average recognition rate (ARR) for all cell types. The methods with Gabor descriptors outperformed all the other non-Gabor descriptors with the minimum of 6.6% and the maximum of 62.76% in ARR. Among the Gabor filter based methods, the proposed method outperforms them by at least 0.72% and at most 24.09%. The histogram based features were not able to distinguish attached and dynamically blebbing cells. As a result, the ten-fold accuracy of the attached cells was 0% for all histogram based features. We also tested the proposed features with nearest-neighbor (NN) method, and it yielded 83.95% in ARR [16]. The SVM outperformed NN by 2.73%.

5. CONCLUSIONS

In this paper, we used SVM with bio-inspired one-against-all model and feature vector derived from Gabor statistics for multi-class classification. In term of accuracy, the Gabor with statistical descriptors methods outperformed all other comparison methods as shown in Table 2. In term of feature vector size, the proposed approach has only 40 descriptors which is less than a single histogram that contains 256 descriptors. In term of reliability, the ten-fold average recognition rate of the proposed method is differed from the predicted accuracy under optimal frequency shown in Fig. 4 by less than 0.2%.

6. ACKNOWLEDGEMENT

This research was supported by NSF-IGERT: Grant DGE 0903667 and by TRDRP: Grant 20XT-0118 and 20FT-0084.

7. REFERENCES

[1] J. A. Thomson, J. Itskovitz-Eldor, S. S. Shapiro, M. A. Waknitz, J. J. Swiergiel, V. S. Marshall and J. M. Jones, "Embryonic stem cell lines derived from human blastocysts," *Science*, vol. 282, no. 5395, pp. 1145-1147, 1998.

[2] Z. Zhu and D. Huangfu, "Human pluripotent stem cells: an emerging model in developmental biology," *Development*, vol. 140, pp. 705-717, 2013.

[3] P. Talbot and S. Lin, "Mouse and human embryonic stem cells: can they improve human health by preventing disease?," *Current Topics in Medicinal Chemistry*, vol. 11, no. 13, pp. 1638-1652, 2011.

[4] S. Lin, V. Tran and P. Talbot, "Comparison of toxicity of smoke from traditional and harm reduction cigarettes using embryonic stem cells as a novel model for pre-implantation development," *Human Reproduction*, vol. 24, pp. 386-397, 2009.

[5] S. Lin, S. Fonteno, J-H Weng, and P. Talbot, "Comparison of toxicity of smoke from conventional and harm reduction cigarettes using human embryonic stem cells," *Toxicological Sciences*, vol. 118, pp. 202-212, Aug. 2010.

[6] S. Lin, S. Fonteno, S. Satish, B. Bhanu and P. Talbot, "Video bioinformatics analysis of human embryonic stem cell colony growth," *Journal of visualized experiments*, vol. 39, May 2010.

[7] T. Ojala, M. Pietikäinen and T. Mäenpää, "Gray scale and rotation invariant texture classification with local binary patterns," *Proc. ECCV*, vol. 1842, pp. 404-420, 2000.

[8] J. Heikkila, V. Ojansivu and E. Rahtu, "Improved blur insensitivity for decorrelated local phase quantization," *International Conference on Pattern Recognition*, pp. 818-821, 2010.

[9] I. Fogel and D. Sagi, "Gabor filters as texture discriminator," *Biol. Cybern.*, vol 61, pp. 103-113, 1989.

[10] W. K. Kong, D. Zhang and W. Li, "Palmprint feature extraction using 2-D Gabor filters," *Pattern Recognition*, vol. 36, pp. 2339-2347, 2003.

[11] C. Chang, C. Lin and C. J. Lin, "LIBSVM: a library for support vector machines," 2001, Available Online: http://www.csie.ntu.edu.tw/~cjlin/libsvm.

[12] O. Chapelle, P. Haffner and V. Vapnik, "SVMs for histogram-based image classification," *IEEE transactions on Neural Networks*, vol. 10, no. 5, pp. 1055-1064, 1999.

[13] R.C. Gonzalez and R.E. Woods, Digital Image Processing: Third Edition. Upper Saddle River, NJ: Pearson Education Inc., pp. 795-856, 2008.

[14] Nikon. Biostation-IM. http://www.nikoninstruments.com/content/search?SearchText=Biostation+IM (accessed 22 Jan. 2014).

[15] B.X. Guan, B. Bhanu, P. Talbot, & S. Lin, "Automated human embryonic stem cell detection," *Proc. 2nd IEEE International Conf. On Health Informatics, Imaging and System Biology*, pp. 75-82, Sept. 2012.

[16] J. H. Friedman, J. Bentely and R. A. Finkel, "An algorithm for finding best matches in logarithmic expected time," *ACM Trans. On Mathematical Software*, vol. 3, No. 3, pp. 209- 226, 1977.